Received: 4 July 2016 | Revised: 12 January 2017 | Accepted: 15 January 2017

DOI: 10.1002/tox.22395

RESEARCH ARTICLE

WILEY ENVIRONMENTAL TOXICOLOGY

The aflatoxin B_1-fumonisin B_1 toxicity in BRL-3A hepatocytes is associated to induction of cytochrome P450 activity and arachidonic acid metabolism

Verónica S. Mary | Silvina L. Arias | Santiago N. Otaiza | Pilar A. Velez | Héctor R. Rubinstein | Martín G. Theumer

Departamento de Bioquímica Clínica, Facultad de Ciencias Químicas, Universidad Nacional de Córdoba, Centro de Investigaciones en Bioquímica Clínica e Inmunología (CIBICI), UNC, CONICET, Córdoba, X5000HUA, Argentina

Correspondence
Martín G. Theumer, Centro de Investigaciones en Bioquímica Clínica e Inmunología (CIBICI), UNC, CONICET, Departamento de Bioquímica Clínica, Facultad de Ciencias Químicas, Universidad Nacional de Córdoba, Haya de la Torre y Medina Allende, Ciudad Universitaria, X5000HUA Córdoba, Argentina.
Email: mgtheumer@fcq.unc.edu.ar

Funding Information
Secretaría de Ciencia y Tecnología-Universidad Nacional de Córdoba; Agencia Nacional de Promoción Científica y Tecnológica, Grant numbers: PICT 2010-1232, 2012-1742, 2013-0750, and 2015-2810; Consejo Nacional de Investigaciones Científicas y Técnicas (CONICET-Argentina).

Abstract

Human oral exposure to aflatoxin B_1 (AFB_1) and fumonisin B_1 (FB_1) is associated with increased hepatocellular carcinoma. Although evidence suggested interactive AFB_1–FB_1 hepatotoxicity, the underlying mechanisms remain mostly unidentified. This work was aimed at evaluating the possible AFB_1–FB_1 interplay to induce genetic and cell cycle toxicities in BRL-3A rat hepatocytes, reactive oxygen species (ROS) involvement, and the AFB_1 metabolizing pathways cytochrome P450 (CYP) and arachidonic acid (ArAc) metabolism as ROS contributors. Flow cytometry of stained BRL-3A hepatocytes was used to study the cell cycle (propidium iodide), ROS intracellular production (DCFH-DA, HE, DAF-2 DA), and phospholipase A activity (staining with bis-BODIPY FL C11-PC). The CYP1A activity was assessed by the 7-ethoxyresorufin-O-deethylase (EROD) assay. Despite a 48-h exposure to FB_1 (30 μM) not being genotoxic, the AFB_1 (20 μM)-induced micronucleus frequency was overcome by the AFB_1–FB_1 mixture (MIX), presumably showing toxin interaction. The mycotoxins blocked G1/S-phase, but only MIX caused cell death. Overall, the oxidative stress led these alterations as the pretreatment with N-acetyl-l-cysteine reduced such toxic effects. While AFB_1 had a major input to the MIX pro-oxidant activity, with CYP and ArAc metabolism being ROS contributors, these pathways were not involved in the FB_1-elicited weak oxidative stress. The MIX-induced micronucleus frequency in N-acetyl-L-cysteine pretreated cells was greater than that caused by AFB_1 without antioxidants, suggesting enhanced AFB_1 direct genotoxicity probably owing to the higher CYP activity and ArAc metabolism found in MIX. The metabolic pathways modulation by AFB_1–FB_1 mixtures could raise its hepatocarcinogenic properties.

KEYWORDS
CYP1A, genotoxicity, mycotoxin mixture, oxidative stress, phospholipase A

1 | INTRODUCTION

Mycotoxins are fungal metabolites commonly found as low-level contaminants of food and feed, which affect human and animal health. Exposure to multiple toxic fungal metabolites through the consumption of varied diets and of foodstuffs naturally contaminated with two or more mycotoxins is a cause of great worldwide concern because their individual toxicities may be modified in a synergistic, additive, or antagonistic manner when they co-occur.[1]

The isolation of *Aspergillus flavus* and *Fusarium verticillioides* and the co-occurrence of their main mycotoxins aflatoxin B_1 (AFB_1) and fumonisin B_1 (FB_1) in the same substrate have frequently been reported, especially in corn and rice, which represent the basic ingredients of human and animal feeding in developing countries.[2,3] The interaction between AFB_1 and FB_1 is a matter of great interest because

Abbreviations: AFB_1, aflatoxin B_1; AFBO, AFB_1-exo-8,9-epoxide; AhR, aryl hydrocarbon receptor; ArAc, arachidonic acid; CAT, catalase; CIP, ciprofloxacin; CYP, cytochrome P450; DEX, dexamethasone; FB_1, fumonisin B_1; HCC, hepatocellular carcinoma; LOX, lipoxygenase; MDA, malondialdehyde; MIX, AFB_1-FB_1 mixture; MN, micronucleus; NAC, N-acetyl-l-cysteine; $O_2^{\cdot-}$, superoxide radical anion; PHS, prostaglandin H synthase; PLA, phospholipase A; RNS, reactive nitrogen species; ROS, reactive oxygen species.

co-exposure to both mycotoxins has been associated with a high incidence of hepatocellular carcinoma (HCC) in humans.[4,5]

AFB_1 is one of the most relevant mycotoxins due to its high toxic potential, being hepatotoxic, immunosuppressive, mutagenic, genotoxic, and carcinogenic in humans and animals.[1,6] The toxicology of this mycotoxin is intimately linked with its biotransformation to the highly reactive AFB_1-*exo*−8,9-epoxide (AFBO), which produces a direct genotoxicity through the formation of adducts with the DNA,[6] and to a lesser extent the induction of oxidative stress, which is responsible (probably among other causes) for the indirect genotoxicity of this aflatoxin.[7] The predominant site of the AFB_1 metabolism is the liver through cytochrome P450 (CYP) activity, with CYP1A2 and 3A4 being the major human CYP isoenzymes involved in AFBO formation.[6] Several studies carried out with liver microsomes of human, chicken, quail, and turkey, and also on human lung cells and lymphoblasts exposed to the concentrations of AFB_1 commonly detected in food, have shown that AFBO formation and DNA damage are mostly induced by CYP1A2.[8–12] Moreover, CYP activity itself is associated with electron leakage, leading to reactive oxygen species (ROS) generation. Therefore AFB_1 bioactivation by this enzymatic complex would be expected to cause ROS production. Among other AFB_1-metabolizing enzymes are found the lipoxygenases (LOX) and prostaglandin H synthase (PHS), which are major components of the arachidonic acid (ArAc) metabolic cascade.[13] By this pathway, the highly reactive AFBO is formed when peroxyl radicals, reactive intermediates formed by LOX and PHS during the ArAc metabolism, epoxidize the AFB_1 8,9-double bond.[14–16] ArAc release from membranes is the limiting step in this metabolic cascade, and can be triggered by the interaction of membrane-active agents with the cell surface.[17] Authors suggested that AFB_1 can stimulate ArAc release from membranes by inducing phospholipase A2 (PLA2) activity, thereby enhancing its own bioactivation.[14] Furthermore, beacuse ROS are also generated as byproducts during the ArAc metabolite oxidation by PHS and LOX, as well as through activating the ArAc-induced NADPH oxidase,[18] then in addition to the extra stimulus for its own bioactivation, AFB_1 might also increase ROS levels.[19] Although the maximum hepatic LOX and PHS activities are minor compared with those of CYP, the AFB_1 oxidative metabolism by the former can occur at low AFB_1 concentrations, and therefore it may be important in terms of human exposure through consumption of diets naturally contaminated with this aflatoxin.[15]

Consequently, variations in CYP activity, and to a lesser extent in PLA2, LOX, and PHS activities, due to environmental factors or genetic polymorphism, may be important determinants in the propensity of populations to develop HCC after exposure to AFB_1.

FB_1 is the most toxic and abundant fumonisin being hepatotoxic, neurotoxic, nephrotoxic, and immunotoxic in animals, and causing cancer in the esophagus and liver of humans and in the liver and kidney of rodents.[20] Its most recognized mechanism of action is by disrupting the sphingolipid metabolism through inhibiting the ceramide synthase enzyme, which leads to an alteration of the functionality of cell membranes, cell growth, and cell injury.[20] FB_1 can also induce oxidative stress, which may be responsible for indirect genotoxicity of this toxin[21]; however, the mechanisms by which this toxin induces ROS have only begun to be evaluated in recent years[19,22] and are still not clearly understood. In addition, the interaction of FB_1 with biological membranes may introduce perturbations in the environment, which might affect the activity of membrane-bound enzymes.[23]

Although FB_1 is not metabolized by CYP, some authors have shown that this toxin can modulate the activities and/or expression of several CYP, such as 1A, 4A, 2B, 2C11, 2E, and 3A1, in rat liver as well as in human and rat hepatic-derived cell lines.[24–26] Therefore, FB_1 possibly stimulates the AFB_1 metabolism and hence increases its toxicity.

On the other hand, previous studies have reported that depending on the sensitivities of the cell types and animal species, as well as the routes and exposure levels, mycotoxins may have diverse cytotoxic effects. AFB_1 was able to induce apoptosis and/or cell cycle arrest at different phases,[27,28] and FB_1 may cause apoptotic cell death, block cell cycle progression and, in some contexts, inhibit apoptosis and stimulate cell growth.[29] These toxic effects could be related to alteration of the cellular oxidative state as well as to direct and/or indirect genotoxicity induced by AFB_1 and FB_1, because increased ROS levels and DNA damage may affect the signaling pathways involved in cell cycle control and cell survival.[30,31]

Studies with combined AFB_1 and FB_1 revealed that the mixture's main target organ was the liver, where the toxic effects (such as changes in liver weight and hepatic enzymes activities, and severe histopathological lesions) were more marked than those produced by the individual toxins in rats, broiler chickens, rabbits, or trout.[32–35] However, the type, complexity, and mechanisms of AFB_1–FB_1 interaction need to be elucidated to clarify the adverse health and environmental effects of these toxin mixtures and to subsequently provide adequate worldwide regulation concerning mycotoxins.

This work was aimed at evaluating the possible interaction of AFB_1 and FB_1 in inducing alteration of the cell cycle and genotoxicity in a rat liver cell line, as well as at elucidating the contribution of oxidative stress to these interactive hepatotoxic effects and the involvement of relevant biochemical pathways metabolizing AFB_1, such as CYP and the ArAc metabolism in ROS generation. The BRL-3A rat liver cells were used in this study because it was demonstrated to be an appropriate tool for testing hepatotoxicity mechanisms such as oxidative stress.[36–38]

2 | MATERIALS AND METHODS

2.1 | Chemicals

Dulbecco's modified eagle medium (DMEM), heat-inactivated fetal bovine serum (FBS), and bovine serum albumin (BSA) were purchased from Gibco Laboratories (Buenos Aires, Argentina), with Bradford reagent being obtained from Bio-Rad Laboratories (Buenos Aires, Argentina). 1,1,3,3-Tetramethoxypropane (TEP), 2-thiobarbituric acid (TBA), 2,4-dinitrophenylhydrazine (DNPH), 2′,7′-dichlorodihydrofluorescein diacetate (DCFH-DA), 4,5-diaminofluorescein diacetate (DAF-2 DA), 7-ethoxyresorufin, AFB_1, β-nicotinamide adenine dinucleotide 2′-phosphate reduced tetrasodium salt hydrate (NADPH), catalase, ciprofloxacin (CIP), cytochalasin-B (Cyt-B), dexamethasone (DEX), dicumarol,

dimethyl sulfoxide (DMSO), ethylene glycol-tetraacetic acid (EGTA), FB_1, gentamicin, guanidine hydrochloride, hydroethidine (HE), L-Glutamine, *N*-acetyl-L-cysteine (NAC), propidium iodide (PI), resorufin, RNAse A, tetramethylrhodamineethyl ester (TMRE), trichloroacetic acid (TCA), trypan blue, and trypsin were purchased from Sigma-Aldrich (Buenos Aires, Argentina). L-α-Phosphatidylserine (PS) was provided by Avanti Polar Lipids (Alabaster, AL, USA). Bis-BODIPY FL C11-PC was purchased from Thermo Fisher Scientific (Buenos Aires, Argentina). All other chemicals were provided by Sintorgan (Buenos Aires, Argentina) at the highest analytical grade available.

2.2 | Cell culture

The BRL-3A immortal rat liver cell line was obtained from the American Type Culture Collection (ATCC) (Manassas, VA, USA). This cell line was cultured in DMEM supplemented with 10% FBS, 1% L-glutamine, and 50 μg/mL gentamicin at 37°C in a humidified atmosphere with 5% CO_2, and split weekly with 0.5% trypsin/0.02% $EDTANa_2$.

For all assays, the BRL-3A cells were plated in Petri dishes (10 cm in diameter) or 24-well plates at a density of 7.2×10^5 cells/dish or 6×10^4 cells/well, respectively.

After 24 h, the cells were treated with 20 μM AFB_1 dissolved in DMSO (final concentration: 8 mM), 30 μM FB_1 dissolved in PBS, or with an AFB_1–FB_1 mixture (20 μM AFB_1 + 30 μM FB_1, MIX). The choice of the higher concentration for FB_1 related to AFB_1 has been made on the basis of the maximum permissible levels of these mycotoxins in the international food standards and on the intestinal AFB_1 and FB_1 absorption (about 100 and 4%, respectively) after oral administration to rats. Moreover, the doses were selected on the basis of the literature data and previous studies.[19,21,25,37]

2.3 | Cell viability

The cell viability was studied after 48 h of incubation with the mycotoxins or DMSO (0.07–0.21%, v/v), using the trypan blue exclusion and MTT tests.[19]

2.4 | Micronucleus (MN) assay

This assay was performed as previously informed by Theumer et al.[21] In brief, the BRL-3A cells were exposed to the toxins for 24 h, and then Cyt-B (3 μg/mL) was added and the cells were incubated for a further 24 h. To assess the ROS involvement in DNA damage, the cells were pretreated with the antioxidant NAC 5 mM for 0.5 h; then the mycotoxins were added and the incubation maintained for 48 h. Afterward, the cells were harvested and fixed for 10 min in absolute methanol, prior to being stained with Hoechst dye. One thousand binucleated cells were analyzed by fluorescence microscopy using an inverted microscope (Nikon, Germany) and MN frequencies were calculated.

2.5 | Cell cycle analysis

The cell cycle was studied by staining with PI and flow cytometric determination.[39] Briefly, the BRL-3A cells were pretreated with or without 5 mM NAC for 0.5 h, to assess ROS involvement in cell cycle alteration. Then, the mycotoxins were added, and after 48 h of incubation, the cells were fixed in 70% ice-cold ethanol overnight at 4°C, before being incubated with 50 μg/mL PI and 100 μg/mL RNase A for 0.5 h at 37°C in the dark. Cells were analyzed using a flow cytometer (FACSCantoII, Becton Dickinson) and 50,000 events were acquired for each sample (excitation at 488 nm, emission at 600 nm). The cellular DNA profile was evaluated using histograms, and the cell percentages of the sub G0/G1 (dead cells), G0/G1, S, and G2/M phases were obtained using software from Verity ModFit 3.1 (Portland, OR, USA).

2.6 | p53 expression

It was assessed by Western blot. BRL-3A cell protein extracts were prepared in sample buffer containing 60 mM Tris–HCl pH 6.8, 10% glycerol, 2% sodium dodecyl sulphate, 1% 2-β-mercaptoethanol, and 0.002% bromophenol blue. Then, the protein samples were separated on a 10% SDS-polyacrylamide gel, and transferred to a nitrocellulose membrane (Amersham Bioscience, Amersahm place, Little Chalfont, UK). Ponceau staining (0.2% Ponceau, 3% tricloroactic acid, 3% sulfosalicilic acid) was used to verify protein transference from gel to nitrocellulose membrane. Nonspecific binding was blocked with 5% nonfat milk in Tris–HCl saline buffer containing 0.01% Tween 20, pH 8.3 (TBS-T) for 1 h at room temperature. The membrane was subsequently incubated with anti-p53 and anti-β-actin (used as loading control) antibodies (Santa Cruz Biotechnology, CA) diluted in 5% nonfat milk in TBS-T at 4°C overnight, washed three times with TBS-T, and then incubated with secondary horseradish peroxidase-conjugated antibodies (Santa Cruz Biotechnology, CA) in TBS-T for 1.5 h at room temperature. The specific band was revealed by a chemiluminescence reaction (Amersham Biosciences) with autoradiographic or maximum performance light films (Kodak, Rochester, NY) and quantified by densitometric analysis using image software (Gel-Pro Analyzer version 3.1).

2.7 | Mitochondrial membrane potential (ΔΨm) assay

To evaluate changes in ΔΨm, the BRL-3A cells were exposed to the mycotoxins for 24 h, and then incubation was continued with 50 nM of the fluorescent probe TMRE for another 0.5 h at 37°C. Afterwards, cells were washed and resuspended in PBS, and the TMRE fluorescence was measured by flow cytometry using exitation and emission wavelengths of 488 and 574 nm, respectively (20,000 events were acquired for each sample). Results were expressed as the relative TMRE mean fluorescence intensity (fold) in treated cells with respect to the untreated ones.

2.8 | Detection of biomolecular oxidative damage

2.8.1 | Proteins

Protein oxidation was determined by measuring the levels of the carbonyl groups, using the spectrophotometric DNPH method as previously described.[19] Briefly, after treatments with the mycotoxins for 48 h, the BRL-3A cells were lysed with 50 mM HEPES buffer (pH 7.4)

containing protease inhibitors. Then, the samples were divided into two equal portions (containing 0.5–1 mg of protein, assessed by the Bradford method), and treated for 1 h with either 10 mM DNPH in 2 M HCl or with 2 M HCl alone. Each portion was washed with ethanol:ethyl acetate (1:1) and dissolved with 6 M guanidine hydrochloride. The carbonyl levels were obtained from the difference in absorbance at 375 nm ($\varepsilon = 22{,}000$ M/cm) between the DNPH-treated and HCl-treated portions, and expressed as nmol of carbonyls/mg protein.

2.8.2 | Lipids

The malondialdehide (MDA) level, a widely used lipid peroxidation marker, was selectively measured by using the TBA test, with subsequent separation and quantification of the MDA–TBA adducts by HPLC.[19] In brief, after exposure to the mycotoxins for 48 h, the BRL-3A cells were lysed with 50 mM HEPES buffer (pH 7.4), and the proteins of the lysates were measured by the Bradford method and precipitated with 5% trichloroacetic acid (TCA).

Samples were treated with 0.25% TBA in 0.5 M HCl for 45 min at 90°C, and then ice-cooled and analyzed by HPLC on a C18 column with UV detection (532 nm). The mobile phase used was 50 mM KH_2PO_4 (pH 6.0):methanol (65:35), at a flow rate of 1 mL/min. The MDA levels were calculated from a calibration curve based on the acid hydrolysis of TEP and the reaction with TBA. All results were expressed as nmol MDA/mg protein.

2.9 | Measurement of catalase (CAT) activity

This antioxidant enzyme catalyzes the decomposition of hydrogen peroxide (H_2O_2) to water and O_2. Briefly, after treatments with the mycotoxins for 24 or 48 h, the BRL-3A cells were lysed with 50 mM HEPES buffer (pH 7.4) containing protease inhibitors. Then, cell debris was removed by centrifugation (11,000g × 10 min at 4°C), and the proteins of the lysates were measured by the Bradford method. CAT activity was measured using the method of Aebi,[40] with 10 μL of each supernatant being mixed with 50 μL of PBS and 40 μL of 0.2 M H_2O_2 per well in a 96-well plate (flat bottom). Finally, 200 μL of 0.2 M potassium dichromate in glacial acetic acid were added to each well and this was maintained for 20 min at 37°C in the dark. The evaluation of enzyme activity was performed by interpolating the absorbance of the samples at 570 nm (determined using the Bio-Rad Benchmark Microplate Reader) on a calibration curve, made with different concentrations of pure CAT plus the reagents mentioned above. The results were expressed as the relative catalase activity (fold) in treated cells with respect to the untreated ones.

2.10 | Detection of ROS and reactive nitrogen species (RNS)

The intracellular production of total ROS, superoxide radical anion ($O_2^{\cdot-}$), and RNS was determined using the probes DCFH-DA, HE, and DAF-2 DA, respectively. Briefly, the BRL-3A cells were exposed to the mycotoxins for 0.5, 4, or 24 h, and then incubation was continued with 10 μM DCFH-DA, 2 μM HE, or 10 μM DAF-2 DA for another 20 min. Afterward, cells were washed and resuspended in PBS, and the fluorescence of the oxidized probes DCF, 2-OH-E+, and DAF-2T, respectively, was measured by flow cytometry (20,000 events were acquired for each sample; with excitation at 488 nm and emission at 528, 580, and 538 nm for DCF, 2-OH-E+, and DAF-2T, respectively). Results were expressed as the relative mean fluorescence intensity (fold) in treated cells with respect to the untreated ones, and as the average percentage of positive cells obtained from a marker used as cutoff to compare the effects, chosen based on the histogram of unstained cells.

To assess the contribution of the CYP monooxygenase system and the ArAc metabolism to ROS formation, the BRL-3A cells were preincubated for 0.5 h with or without 50 μM CIP (inhibitor of main CYP isoenzymes metabolizing AFB_1, 1A, and 3A)[41] or 0.01 μM DEX (PLA2 inhibitor).[42] Then, the mycotoxins were added to the medium, and the cells were maintained in the culture for 24 h and treated with 10 μM DCFH-DA, as explained above.

2.11 | Measurement of PLA activity

The PLA activity was monitored using a synthetic fluorogenic phospholipid molecule bis-BODIPY FL C11-PC, which is cleaved by PLA resulting in unquenching and green fluorescent emission. Briefly, the probe (1 mg/mL dry chloroform) was combined with PS (2 mg/mL dry chloroform) in a molar ratio 1:9, and then, the organic solvent was evaporated under a stream of nitrogen. After, the dried lipid film was rehydrated with 1 mL PBS and sonicated using a probe sonicator for 30 min (90 W power) on ice, to obtain small unilamellar liposomes. Promptly, the labeled liposomes and BRL-3A cells were mixed at a ratio of 0.2 μg probe/5 × 10^5 cells in 50 μL PBS containing 0.1% BSA and incubated for 60 min a 37°C, to incorporate the probe into the plasma membrane inner leaflet via fusion with labeled PS liposomes. Then, the cells were washed three times in PBS and resuspended in PBS containing 1.5 mM Ca^{2+}/1.5 mM Mg^{2+}, pH 7.3, for 10 min at 37°C. At the end of the incubation period, the reaction was stopped by adding an ice-cold solution containing 2 mM EGTA, 150 mM NaCl, and 1% BSA-free fatty acid. Cells were analyzed using a flow cytometer and 20,000 events were acquired for each sample (excitation at 488 nm and emission at 530 nm). Results were expressed as the relative bis-BODIPY FL C11-PC mean intensity of fluorescence (fold) in treated cells with respect to the untreated ones.

2.12 | Assessment of the CYP1A activity

The 7-ethoxyresorufin-O-deethylase (EROD) assay was used to estimate the activity of CYP1A.[25] Briefly, the BRL-3A cells exposed to the treatments with mycotoxins for 24 h were washed with PBS (pH 7.5) and frozen in liquid nitrogen. Then, a reaction mixture containing buffer Na_2HPO4 (50 mM, pH 8.0), 7-ethoxyresorufin (1.25 μM), dicumarol (20 μM), and NaDPH (0.5 mM) was added to each sample. The resorufin product formation was measured at 532 nm excitation and 590 nm emission wavelengths in a Multi-Mode Microplate Reader Sinergy HT (BioTek Instruments, Winooski, VT, USA). Resorufin concentrations were determined from a calibration curve in the range of 0–50 pmol of

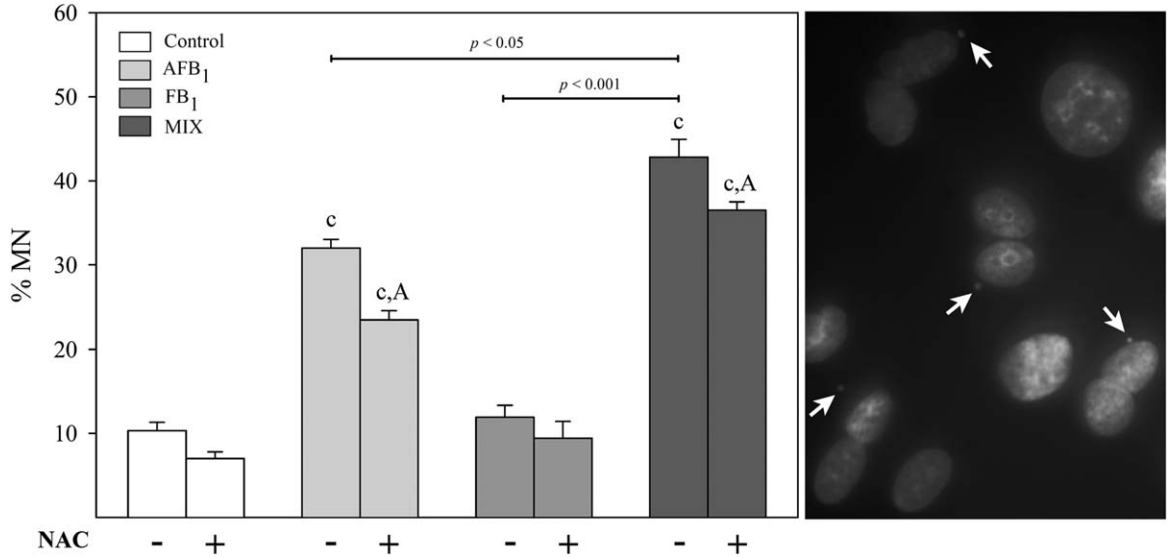

FIGURE 1 DNA damage induced by individual and combined AFB_1 and FB_1 in BRL-3A cells at 48 h: involvement of oxidative stress. The results are expressed as % MN. Lowercase letters indicate differences from the corresponding control ($^{c}P < 0.001$). Capital letters denote the differences between the treatments with and without NAC ($^{A}P < 0.05$). (Right) Fluorescent micrograph of binucleated cells after treatment with MIX and cytochalasin-B, showing MN with Hoechst stain

resorufin standard, and then were normalized per milligram protein from the BSA standard curve as determined by the Bradford method. EROD activity was expressed as pmol resorufin/mg protein/min.

2.13 | Statistical analysis

Data from these studies were obtained from a minimum of three independent experiments ($n = 6$, for each treatment), and assessed by a one-way ANOVA followed by Bonferroni's post hoc test using GraphPadInStat software version 3.01 (La Jolla, CA, USA). Results were expressed as the mean ± standard error of the mean (SEM), with differences being considered significant at the $P < 0.05$ level.

3 | RESULTS

3.1 | Cell viability

The trypan blue exclusion and MTT tests showed that the cell viability at 48 h was in the range 80–90% depending on the treatment with mycotoxins and was above 90% in the control cells (data not shown).

3.2 | DNA damage induced by AFB_1 and FB_1

Among the available genotoxicity tests, MN assay is recognized due to its robustness, sensitivity, and statistical power to evaluate DNA breaks, which can be considered hallmarks of mutagenicity.[43] The ability of individual and combined mycotoxins to induce DNA damage in BRL-3A cells was tested at 48 h and the presence of MN was evidenced by Hoechst staining (Figure 1). The incubation of cells with AFB_1 and MIX significantly raised the frequency of MN compared to control (the changes were higher than three- and fourfold, respectively), whereas exposure to FB_1 did not produce significant changes in the basal DNA damage observed in the absence of toxins. There was a higher percentage of MN in cells treated with MIX, compared to the AFB_1 or FB_1 treatments. Furthermore, the effect caused by AFB_1 alone or combined with FB_1 was partially inhibited by the antioxidant NAC ($P < 0.05$ in both cases).

3.3 | Cell cycle arrest induced by AFB_1 and FB_1

As it is widely known that the DNA damage is often accompanied by cell cycle arrest, the AFB_1 and FB_1 effects on the cell cycle were tested in the BRL-3A cells, with results of these experiments being shown in

TABLE 1 Cell cycle alteration induced by individual and combined AFB_1 and FB_1 in the BRL-3A cells at 48 h: involvement of oxidative stress

Treatment	NAC	G0/G1	S	G2/M
Control	−	65.28 ± 0.22	30.67 ± 0.40	4.10 ± 0.15
	+	64.00 ± 0.40	32.00 ± 0.35	4.30 ± 0.19
AFB_1	−	69.85 ± 0.39***	26.64 ± 0.46***	3.40 ± 0.23
	+	67.50 ± 0.28***#	29.00 ± 0.40**#	3.70 ± 0.17
FB_1	−	69.45 ± 0.39**	27.25 ± 0.53**a	3.50 ± 0.20
	+	68.00 ± 0.57**	28.60 ± 0.50**	3.60 ± 0.15
MIX	−	71.00 ± 0.60***	25.00 ± 0.49***	3.40 ± 0.19
	+	67.00 ± 0.46**##	28.50 ± 0.46**##	3.80 ± 0.22

Results are expressed as average cell percentage in each phase ± SEM.
*Difference from the corresponding control (**$P < 0.01$, ***$P < 0.001$).
#Difference between the treatments with and without NAC (#$P < 0.05$, ##$P < 0.01$). Letters indicate differences between the MIX and mycotoxins alone ($^{a}P < 0.05$).

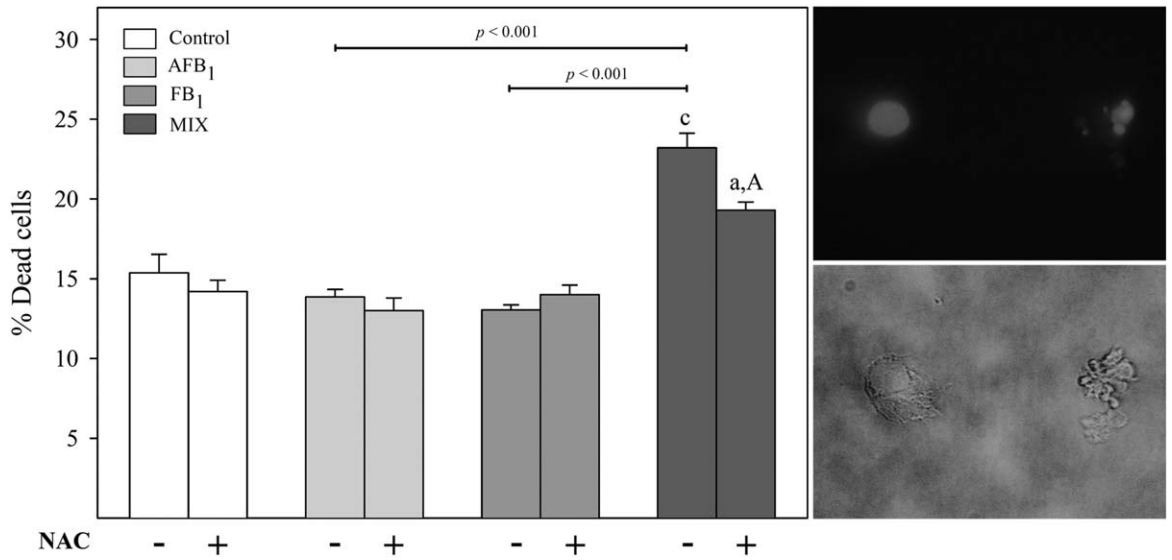

FIGURE 2 Cell death induced by individual and combined AFB_1 and FB_1 in BRL-3A cells at 48 h: involvement of oxidative stress. The results are expressed as % dead cells. Lowercase letters indicate the differences from the corresponding control ($^aP < 0.05$, $^cP < 0.001$). Capital letters denote the differences between the treatments with and without NAC ($^AP < 0.05$). (Right) Fluorescent micrograph of cells treated with MIX, showing apoptotic cell death with Hoechst stain, and the corresponding bright field image

Table 1. The percentages of cells in the G0–G1 and S phases were either increased or decreased, respectively, after treatments for 48 h with MIX, AFB_1 ($P < 0.001$ in both cases) or FB_1 ($P < 0.05$). Nevertheless, there were no significant differences among the treatments with the mycotoxins, except for the lower proportion of cells in the S phase found in MIX compared to FB_1 ($P < 0.05$).

To assess whether DNA oxidative damage had contributed to the minor G1–S phase transition, the cells were pretreated with NAC, and it was found that this antioxidant significantly decreased the G1-phase arrest caused by AFB_1 ($P < 0.05$) and MIX ($P < 0.01$).

3.4 | Cell death induced by AFB_1 and FB_1

A decrease in DNA content was used as cell death marker, which was measured by flow cytometry in the BRL-3A cells treated with mycotoxins for 48 h. The findings of these assays are depicted in Figure 2, which shows that MIX was the only treatment that significantly increased the percentage of dead cells, with respect to either the control or the mycotoxins alone ($P < 0.001$ in all cases). Furthermore, pretreatment with NAC prevented partly the cell death induced by MIX ($P < 0.05$).

Morphological evaluation of cell nuclei showed that the cell death induced by MIX was mainly apoptotic (Figure 2).

3.5 | p53 expression induced by AFB_1 and FB_1

Immunoblotting assay showed that the p53 protein levels in BRL-3A cells increased after 24 h of treatment with mycotoxins individually and especially in combination. Moreover, the higher p53 expressions induced by AFB_1 and MIX were partially prevented when the cells were preincubated with NAC (Figure 3).

3.6 | Mitochondrial membrane depolarization induced by AFB_1 and FB_1

The effect of AFB_1 and FB_1 on the $\Delta\Psi m$ was measured by flow cytometry in the BRL-3A cells treated with mycotoxins for 24 h. The results of these assays (Figure 4) show that the TMRE fluorescence intensity

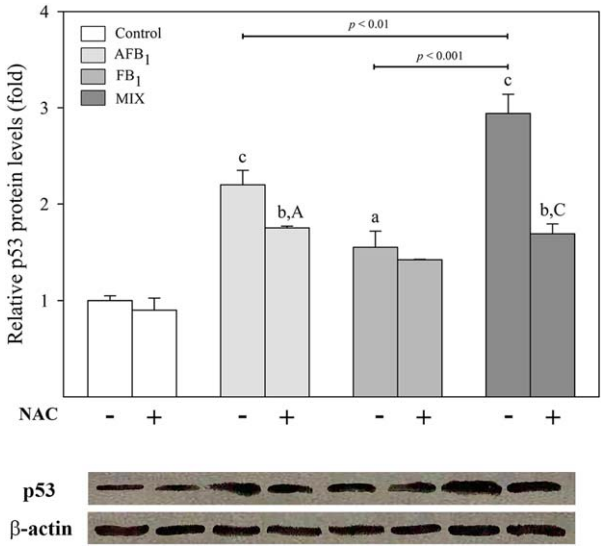

FIGURE 3 p53 protein level induced by individual and combined AFB_1 and FB_1 in BRL-3A cells at 24 h: involvement of oxidative stress. The p53 expression was normalized with the β-actin expression, and the results are expressed as the relative p53 protein level (fold) in treated cells with respect to the untreated ones, with lowercase letters indicating differences from the corresponding control ($^cP < 0.001$), and capital letters denoting differences between the treatments with and without NAC ($^AP < 0.05$). A representative blot is shown

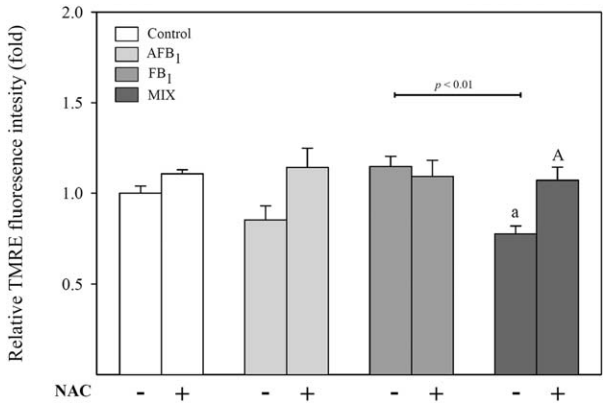

FIGURE 4 Changes in mitochondrial membrane potential induced by individual and combined AFB_1 and FB_1 in BRL-3A cells at 24 h: involvement of oxidative stress. The results are expressed as relative TMRE-fluorescence intensity (fold) in treated cells, with respect to untreated ones. Lowercase letters indicate differences from the corresponding control ($^aP < 0.05$), and capital letters denote differences between the treatments with and without NAC ($^AP < 0.05$)

was decreased in MIX-treated cells ($P < 0.05$), concordantly with the findings in the DNA content analysis, hence confirming the induction of apoptotic cell death. Moreover, pretreatment with NAC prevented the mitochondrial membrane depolarization produced by MIX ($P < 0.05$).

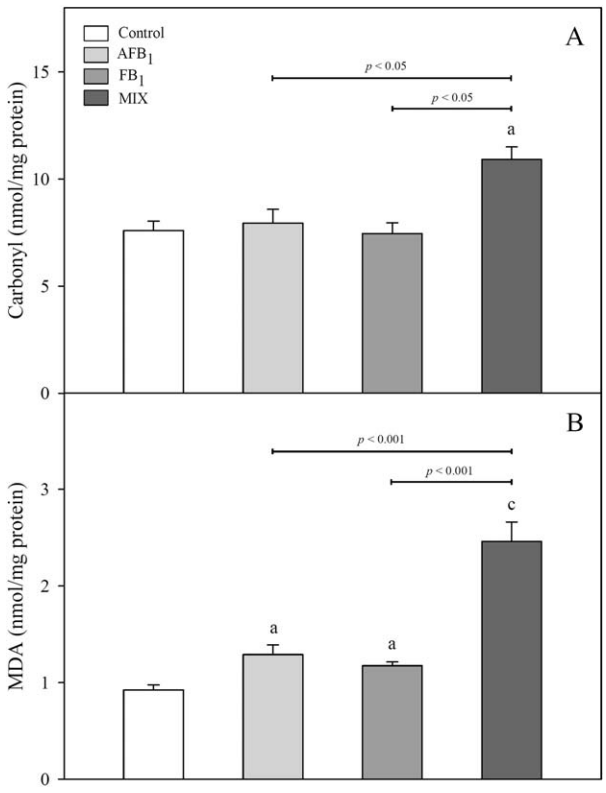

FIGURE 5 Carbonyl (A) and MDA (B) levels induced by individual and combined AFB_1 and FB_1 in BRL-3A cells at 48 h. The results are expressed as nmol carbonyls or MDA/mg of protein. Letters indicate differences from the control ($^aP < 0.05$, $^cP < 0.001$)

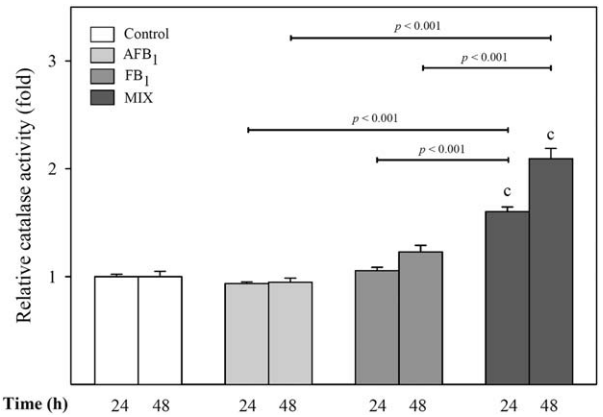

FIGURE 6 Catalase activity induced by individual and combined AFB_1 and FB_1 in BRL-3A cells at 24 and 48 h. The results are expressed as the relative catalase activity (fold) in treated cells with respect to the untreated ones. Letters indicate differences from the corresponding control ($^cP < 0.001$)

3.7 | Biomolecular oxidative damage induced by AFB_1 and FB_1

The protein carbonyl and MDA levels were assessed in BRL-3A cells to estimate the extent of the oxidative damage induced by exposure to the mycotoxins for 48 h (Figure 5) in proteins and lipids, respectively.

MIX was the only treatment that significantly increased the carbonyl levels with respect to control and the mycotoxins alone (Figure 5A). However, exposure of the cells to AFB_1 and FB_1, individually or in combination, significantly raised MDA formation with regard to the control (Figure 5B) with the lipid peroxidation being higher in the cells treated with MIX compared to that with the mycotoxins alone.

3.8 | Effects of AFB_1 and FB_1 on CAT activity

CAT biological activity was measured as an oxidative stress biomarker in the BRL-3A cells exposed to the mycotoxins for 24 and 48 h, with the results being shown in Figure 6.

Although the incubation of the cells with AFB_1 and FB_1 alone did not produce any major changes in the CAT activity, MIX significantly raised this marker of oxidative status compared to control and mycotoxins individually at both end points tested ($P < 0.001$ in all cases).

3.9 | Intracellular RNS generation induced by AFB_1 and FB_1

The ability of mycotoxins to induce intracellular RNS (nitric oxide and its degradation products, such as nitrosonium cation, peroxynitrite anion, and nitrogen dioxide) in BRL-3A cells was tested at 24 h using the DAF-2 DA probe. In Figure 7A, representative histograms of DAF-2T fluorescence intensity are depicted, which display the percentages of positive cells from untreated BRL-3A cells and those incubated with the mycotoxins. In addition, the average percentages for each treatment were calculated from these results.

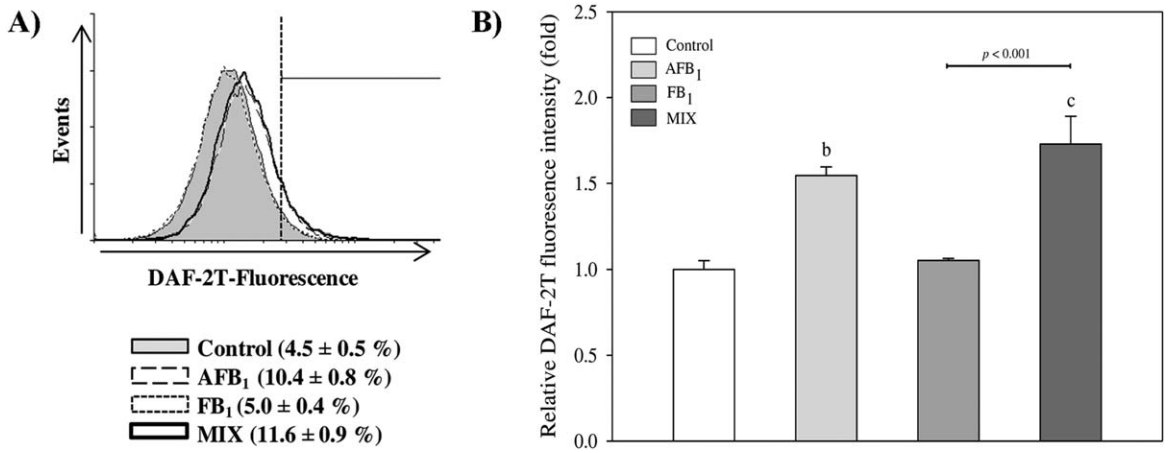

FIGURE 7 The total RNS level induced by individual and combined AFB_1 and FB_1 in BRL-3A cells at 24 h. A, Representative histograms of DAF-2T fluorescence intensity showing percentages of DAF-$2T^+$ cells, and B, relative DAF-2T -fluorescence intensity (fold) in treated cells with respect to untreated ones. Letters indicate the differences from the control ($^bP < 0.01$, $^cP < 0.001$)

In a similar manner, AFB_1 and MIX significantly increased the percentage of DAF-$2T^+$ cells (Figure 7A, $P < 0.001$ for both cases) and relative DAF-2T fluorescence intensities compared to control (Figure 7B). However, FB_1 alone did not modify either of these parameters (Figure 7A,B).

3.10 | Intracellular $O_2^{\cdot-}$ generation induced by AFB_1 and FB_1

The $O_2^{\cdot-}$ levels were measured using the HE probe in BRL-3A cells exposed to the mycotoxins for 0.5 and 4 h. When BRL-3A cells were incubated for 0.5 h with toxins, the $O_2^{\cdot-}$ levels remained unchanged with respect to control (data not shown), whereas $O_2^{\cdot-}$ generation was modulated in cells cultured 4 h with the mycotoxins.

In Figure 8A, representative histograms of HE fluorescence intensity for each treatment are shown, which display the average percentage of positive cells for each experimental condition at 4 h. $O_2^{\cdot-}$ generation increased after MIX, as depicted by the significant rises in the percentage of HE^+ cells (Figure 8A) and in the HE fluorescence intensity (Figure 8B), with respect to control ($P < 0.001$ for both parameters) or the mycotoxins individually ($P < 0.01$ for the two toxins and both parameters). A tendency to higher values than control, although lacking statistical significance, was also induced by AFB_1 and FB_1 alone.

3.11 | Intracellular total ROS generation induced by AFB_1 and FB_1

The capacity of mycotoxins to induce intracellular ROS in the BRL-3A cells was studied at 0.5, 4, and 24 h of incubation by using the DCFH-DA probe. Representative histograms of DCF fluorescence intensity for each treatment are shown in Figure 9A, where the average percentage of positive cells for each experimental condition at 24 h can be observed.

The 24 h exposure of the BRL-3A cells to AFB_1, FB_1 and MIX resulted in significant increases in the proportion of DCF^+ cells (Figure 9A, $P < 0.01$, $P < 0.05$, $P < 0.001$, respectively) and in the relative DCF

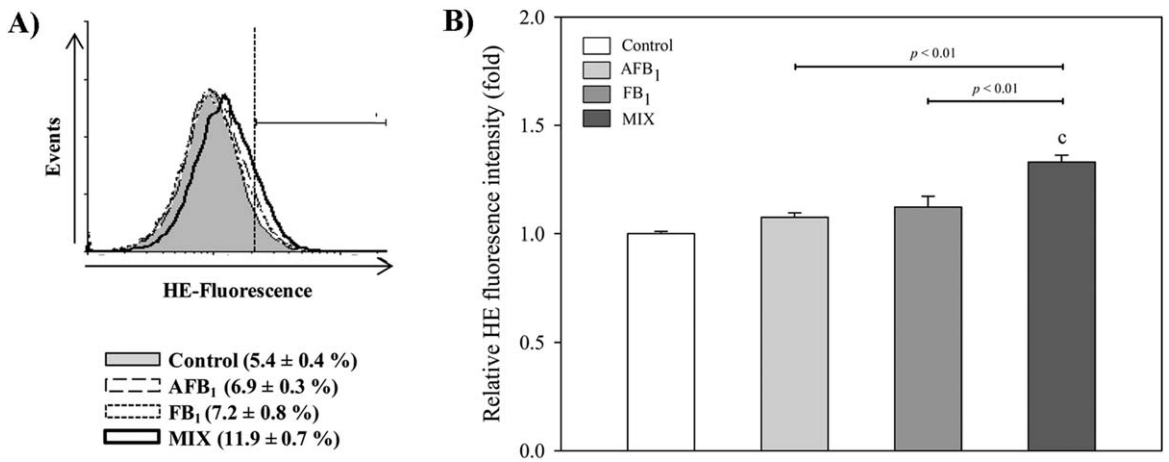

FIGURE 8 The $O_2^{\cdot-}$ level induced by individual and combined AFB_1 and FB_1 in BRL-3A cells at 4 h. Representative histograms of HE fluorescence intensity showing percentages of HE^+ cells (A), and relative HE-fluorescence intensity (fold) in treated cells with respect to untreated ones (B). Letters indicate the differences from the control ($^cP < 0.001$)

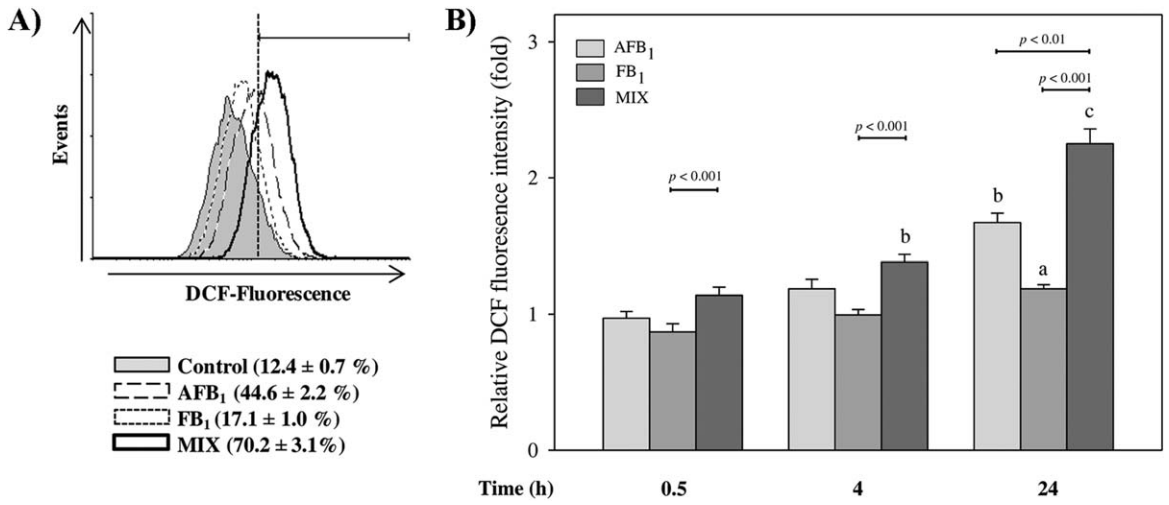

FIGURE 9 The total ROS level induced by individual and combined AFB_1 and FB_1 in BRL-3A cells at 0.5, 4, and 24 h. Representative histograms of DCF fluorescence intensity from cells incubated or not with the mycotoxins for 24 h, showing the percentages of DCF^+ cells (A); and relative DCF fluorescence intensities (fold) in treated cells, with respect to untreated ones (B). Letters indicate the differences from the control ($^aP < 0.05$, $^bP < 0.01$, $^cP < 0.001$)

fluorescence intensity (Figure 9B) compared to control, with ROS levels being higher in the cells treated with MIX compared to the individual mycotoxins ($P < 0.01$ for AFB_1 and $P < 0.001$ for FB_1, for both parameters). However, when the BRL-3A cells were incubated with mycotoxins for shorter times, no differences in the ROS levels were observed with respect to control, except for MIX, which resulted in an enhanced ROS accumulation at 4 h, as depicted by the significant rise in the DCF fluorescence intensity at this end point (Figure 9B, $P < 0.01$).

3.12 | Biochemical pathways involved in the ROS generation induced by AFB_1 and FB_1

Using the DCFH-DA probe, the participation of the ArAc metabolism and the CYP monooxygenase system in the ROS generation was assessed by preincubating the BRL-3A cells with DEX (PLA2 inhibitor) or CIP (CYP 1A and 3A inhibitor), respectively, prior to a further 24 h incubation of the cells with the mycotoxins (Figure 10). AFB_1 increased the DCF fluorescence intensity 0.67-fold change with respect to the control and this raise was decreased in 0.25- and 0.32-fold changes by DEX and CIP, respectively. In contrast, these blocking substances had scarce effects on the DCF fluorescence intensity increased by FB_1, indicating that the ROS sources studied did not significantly contribute to the higher oxidative status induced by this fumonisin. Moreover, both inhibitors significantly prevented the ROS increase induced by MIX, with the DCF fluorescence intensity elicited by MIX + CIP being significantly lower ($P < 0.05$) with regard to that induced by MIX + DEX, and suggesting a greater contribution from the CYP system to ROS accumulation. In other words, MIX caused a rise in the DCF fluorescence intensity of 1.3-fold change relative to control, with this increment being reduced by 0.49- and 0.81-fold changes by DEX and CIP, respectively. These results strongly suggest that the ArAc metabolism and CYP activity significantly contributed to the ROS increase elicited by AFB_1 and MIX, pointing out these metabolic pathways as major ROS sources stimulated by the AFB_1-containing treatments.

3.13 | Effects of AFB_1 and FB_1 on PLA biological activity

PLA biological activity was measured by flow cytometry in the BRL-3A cells exposed to the mycotoxins for 24 h, with representative histograms of bis-BODIPY FL C11-PC fluorescence and the relative mean intensity of fluorescence (MIF) of this probe for each treatment being shown in Figure 11A,B, respectively. AFB_1 and MIX significantly increased the bis-BODIPY FL C11-PC MIF respect to the control ($P < 0.001$, in both cases), with MIX-induced PLA activity being

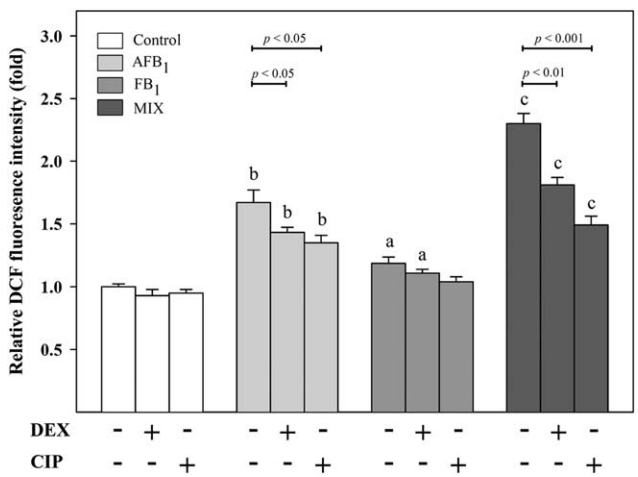

FIGURE 10 Induction of the ArAc metabolism and the CYP monooxygenase system by individual and combined AFB_1 and FB_1 in BRL-3A cells at 24 h. The results are expressed as the relative DCF fluorescence intensity (fold) average in treated cells, with respect to untreated ones. Letters indicate the differences from the corresponding control ($^aP < 0.05$, $^bP < 0.01$, $^cP < 0.001$)

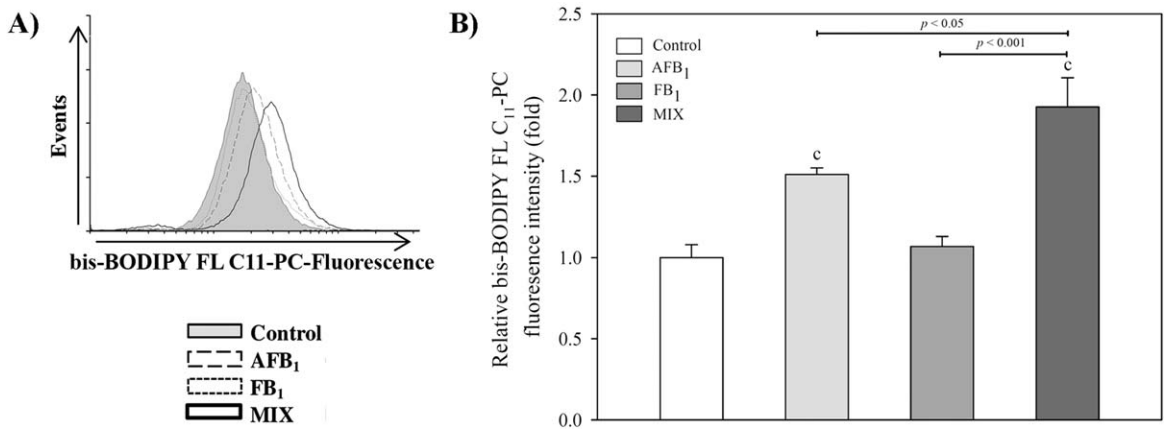

FIGURE 11 The PLA activity induced by individual and combined AFB_1 and FB_1 in BRL-3A cells at 24 h. Representative histograms of bis-BODIPY FL C11-PC fluorescence (A), and relative mean fluorescence intensity (fold) of this probe in treated cells, with respect to untreated ones (B). Letters indicate the differences from the control ($^cP < 0.001$)

significantly higher than the one stimulated by AFB_1 ($P < 0.05$) and FB_1 ($P < 0.001$) individually.

3.14 | Effects of AFB_1 and FB_1 on CYP1A activity

While the exposure of BRL-3A cells to AFB_1 for 24 h resulted in a significant increase of EROD activity ($P < 0.05$), FB_1 did not modify this parameter. However, when cells were cultured with the mixture of both mycotoxins, there was a significant increase in EROD activity with respect to control ($P < 0.001$) and individual mycotoxins ($P < 0.05$ for AFB_1; $P < 0.001$ for FB_1) (Figure 12).

4 | DISCUSSION

In this work, it was found that the AFB_1–FB_1 mixture had higher genotoxic, mutagenic, and cytotoxic effects than those caused by the toxins individually. Although FB_1 did not significantly modify the MN frequency, the genotoxicity resulting from AFB_1 in the BRL-3A cells was increased by its combination with the former toxin, suggesting the probable occurrence of a synergistic interaction between them that could confer a higher hepatocarcinogenic potential to the mixture. These results are in agreement with findings from *in vivo* studies, which showed that the simultaneous subchronic oral administration of AFB_1 and FB_1 to rats produced more liver cancer initiation than the exposure to the individual mycotoxins.[44]

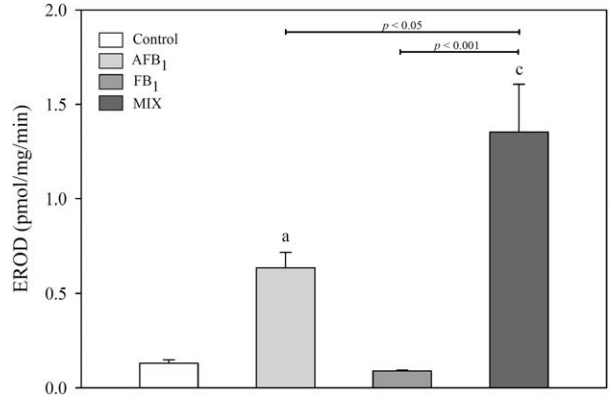

FIGURE 12 CYP1A activity induced by individual and combined AFB_1 and FB_1 in BRL-3A cells at 24 h. Letters indicate the differences from the control ($^aP < 0.05$, $^cP < 0.001$)

AFB_1 and FB_1 individually cause excessive ROS formation,[19,21,29,45] that could readily attack DNA and generate a variety of lesions, such as oxidized DNA bases, abasic sites, and DNA strand breaks, leading ultimately to genomic instability.[46] Hence, we explored the probable involvement of ROS in the chromosome aberrations induced by these mycotoxins, after preincubating the BRL-3A cells with the thiol-containing antioxidant NAC, which has been widely used to investigate the role of ROS in numerous biological and pathological processes, for its free-radical direct scavenging activity and for being a precursor of L-cysteine and reduced glutathione.[47,48] It was found that NAC partially reduced the percentage of MN, and therefore the mutagenicity of the AFB_1–FB_1 mixture, indicating that the genetic damage was produced at least in part by DNA oxidation, which has been previously proposed as an indirect toxicity mechanism exerted by these toxins individually.[21,45] However, due to the nonoxidative genotoxicity found in cells incubated with both toxins being greater than that observed in cells treated only with AFB_1, this may be indicating an increased direct genotoxic activity (adduct formation) of the mixture, probably as a result of the major activation of CYP and the ArAc metabolism, which are the biochemical pathways involved in AFB_1 biotransformation.[13–16] The results of this study are in agreement with those from a previous investigation, where the combination of AFB_1 and FB_1 resulted in increased CYP activity in H4IIE rat hepatoma cells by inducing specifically *cyp1A* expression and CYP1A activity, respect to the individual toxins.[25] Although some studies have shown that FB_1 clastogenicity and genotoxicity were associated with an indirect mechanism involving oxidative damage to the human-derived hepatoma (HepG2) cells, spleen mononuclear cells, and hepatocytes from rat,[19,21,49] FB_1 did not increase chromosomal aberrations in BRL-3A cells, even though the toxin worsened the cellular oxidative status. The lack of changes in the MN frequency in cells exposed to FB_1 could in

fact have been related to several factors, including dose and time of incubation, as well as the intrinsic susceptibility of BRL-3A cells to its toxicity, with all of these contributing to some extent to an efficiently scavenged slight rise in ROS, to an effective DNA repair, or to both.

Genetic alterations can lead to cell cycle arrest, death, or malignant transformation, depending on the lesion severity, cell type, and cellular context.[30] Inhibition of the cell cycle progression in the G1 phase is largely dependent on the activation of the p53 tumor suppressor gene,[50] which may be an adaptive survival process activated to give additional time for DNA repair and to limit the mutations that might arise when replicating damaged genetic material. Alternatively, G1-phase arrest can lead to apoptosis activation.[51] In this study, the blocking in the G1- to S-phase transition, which was correlated to higher expression of p53, might be revealing a cell first attempt to repair genotoxic lesions caused by the mycotoxin mixture. Later, a severely damaged DNA probably exceeding the repair capacities in cells treated with the mycotoxin mixture may have led to membrane depolarization and apoptosis, which plays a crucial role in maintaining genomic integrity by selectively removing the most heavily impaired cells from the population.[30] Despite it was previously reported that FB_1 prevented the mitochondrial membrane depolarization in human gastric cancer MGC-803 cells[52] and in rat primary retinal cultures[53]; in this work, the oxidative stress induced by the mycotoxin combination could be responsible by the mitochondrial membrane depolarization that leads to cell apoptosis. The exposure of BRL-3A cells to AFB_1 and FB_1 individually did lead neither to mitochondrial membrane depolarization nor to cell death, potentially due to nonlethal DNA damage at least partially reverted within the G1-phase arrest induced by the mycotoxins individually. The results of this study are in line with previous ones informed by Sun et al.,[37] who have shown that under similar experimental conditions, AFB_1 and FB_1 individually did not alter the BRL-3A cell viability. Moreover, jointly they could be indicating a relatively higher resistance of these hepatic cells to the toxins, as other authors demonstrated that AFB_1 and FB_1 alone can induce cell death in several cell types.[27,29]

In this work, the oxidative stress was partially responsible for the hepatotoxic effects stimulated by AFB_1 either alone or combined with FB_1 (but not that induced by the individual FB_1), since NAC pretreatment of BRL-3A hepatocytes could only attenuate the blocking of cell cycle progression in the treatments with AFB_1 and the mycotoxin mixture. Oxidative hepatotoxicity may have been produced because an aberrant increase of ROS altered the signaling pathways that modulate the expression of genes such as p53 and others involved in the activation of cell cycle control points and apoptosis.[31,54]The results of this work support the hypothesis of Ricordy et al.,[28] who postulated that the toxic effect of AFB_1 on cell cycle progression may be related to differences in p53 expression, arresting it when a slight DNA damage lets a functional p53 protein synthesis (AFB_1 alone, this work), or inducing cell death in the case of an aberrant gene expression due to extensive genetic damage ($AFB_1 + FB_1$, this work). Moreover, cell cycle arrest and cell death remaining in cells treated with AFB_1 and NAC may be associated with the direct genotoxicity of this toxin.

As AFB_1 and the mixture, FB_1 increased the expression of p53 and caused G1 to S-phase blocking although in an oxidative-stress-independent way. This regulatory protein was probably involved in the cell cycle arrest induced by FB_1; however, the modulated expression and/or activity of some proteins involved in the G1/S checkpoint (such as p21; Cyclin E; Cyclin dependent kinase 2, CDK2; and CDK inhibitors) by this fumonisin might have been involved in such outcome.[55] The already well-documented perturbations of the sphingolipid metabolism produced by this toxin[20] could mediate such effects, as sphingoid base signaling is involved in cell cycle control.[56,57] Nevertheless, the chronological and differential expression of genes controlling cell cycle progression upon exposure to the individually or mixed AFB_1 and FB_1 remains to be explored in depth.

Similar to the observations about the cytotoxic and genotoxic effects, the results from this study suggest a possible synergistic interaction of the toxins to induce oxidative stress. In cells exposed to the AFB_1–FB_1 mixture, this was characterized by an increased oxidation of proteins and lipids, which in turn was correlated with higher accumulations of $O_2^{\cdot-}$ and total ROS, mainly generated by CYP complex activation and increased ArAc metabolism. This treatment also stimulated catalase activity probably as a compensatory mechanism of the increased H_2O_2 and lipid peroxides, which are reactive species that induce the antioxidant enzyme expression.[58]

The results of this work may also indicate a major contribution of AFB_1 to the pro-oxidant activity of the mycotoxin mixture, because cell treatment with this aflatoxin alone also increased lipid oxidation and total ROS content, whose biochemical sources were both the increased CYP activity and the ArAc metabolism. Supporting this, the relative DCF fluorescence intensities, a widely used indicator of total ROS content, were 2.25-, 1.67-, and 1.19-fold greater than control in BRL-3A hepatocytes treated with the mixture, AFB_1 and FB_1, respectively, with even the major ROS sources induced by this fumonisin being different than the ones tested in this study. Furthermore, the rise in RNS observed in cells incubated with the both toxin mixture was also stimulated by AFB_1 alone, but not by the FB_1 treatment. However, it is probable that the contribution of these reactive species to biomolecule oxidation as well as the cytotoxic and genotoxic effects studied is not relevant due to the low cell percentage that increased RNS production (about 10%, for treatments with individual AFB_1 and the mixture), compared to that increasing total ROS production (about 45% and 70% for treatments with AFB_1 single and in combination with FB_1, respectively). In addition, the lack of interactive effect between the toxins in RNS generation is not correlated with the mycotoxin interaction to induce hepatotoxicity, suggesting a scarce or null RNS contribution to such toxicity.

The single mycotoxins were not effective at evoking the protein carbonyl increase produced by their mixture. In fact, the oxidative stress induced by these toxins would stimulate proteasome-dependent degradation of oxidized proteins, thus decreasing protein carbonyl to basal levels. Notwithstanding, a more severe oxidative stress triggered by the mycotoxin mixture could provoke extensive oxidation, thereby generating cross-linked and aggregated proteins that become resistant

to proteolysis and cause accumulation of cytotoxic protein oxidation products.[59,60] Excessive protein oxidation may also have a wide range of functional consequences, such as inactivation of DNA repair enzymes, loss of DNA polymerase fidelity and modification of the protein activity involved in proliferation, cell cycle and death, which may promote genotoxicity and carcinogenicity.[61] Favoring such outcomes, the lipid peroxidation caused mainly by the mixture, but also by the individual mycotoxins, probably contributes to their genotoxic and cytotoxic effects. Some lipid peroxidation products, such as MDA and 4-hydroxynonenal (4-HNE), which are generated by the nonenzymatic or enzymatic decomposition of ArAc and larger PUFAs,[62] can covalently react with DNA, proteins, and lipids, thus leading to DNA strand breaks, mutations, loss of membrane fluidity, cell cycle arrest, and apoptosis.[63,64] Nevertheless, a major contribution of the lipid peroxidation to the genotoxicity and cytotoxicity of the mycotoxin mixture would be expected, owing to the greater ArAc metabolism induced by this treatment.

In this work AFB_1 alone, and especially combined with FB_1, increased the activity of PLA and CYP1A, being the latter in agreement with previous results published by Mary et al.[25] The interactive effects of the AFB_1–FB_1 mixture on the CYP activity and ArAc metabolism induction may have been associated with the higher oxidative stress caused by the combined action of both mycotoxins, with the data indicating the nuclear transcription factor aryl hydrocarbon receptor (AhR) as being the probable mediator of such actions. Recently, Mary et al.[25] postulated that AFB_1 is an AhR agonist, as it increased the CYP1A activity and *cyp1A* transcription in the H4IIE rat hepatoma cell line, which was associated with an enhanced AhR activity (a primary regulator of *cyp1A* expression) in DR-CALUX cell line. Moreover, the induction of other CYP subfamilies such as 3A by AFB_1[65] and FB_1,[24] as well as the AFB_1 metabolization itself by CYP, might also contribute to the higher activity of this enzyme complex and consequent ROS generation. On the other hand, the increased ArAc metabolism could be secondary to a major *PLA2* expression caused by toxin-stimulated AhR signaling, as previous genome microarray and real-time quantitative RT-PCR studies have demonstrated increased *PLA2* mRNA levels upon AhR activation in mouse liver and hepatoma Hepa-1c1c7 cells.[66,67] Taken together, the preceding data suggest that the stronger induction effect of the AFB_1–FB_1 mixture on the metabolic pathways studied in this study was probably provoked by a higher AhR activation, similarly to that observed in hepatic H4IIE cells.[25]

In summary, the results presented in this work show that exposure to the AFB_1–FB_1 mixture increased the ArAc metabolism and CYP activity in BRL-3A hepatocytes, leading to higher ROS synthesis and subsequent stronger oxidative biomolecular damage. Furthermore, this study strongly suggests that the AFB_1–FB_1 mixture could be raising the AFBO generation by the increased activity of such AFB_1 metabolizing pathways. Together, the enhanced AFB_1 bioactivation and the induction of a greater oxidative stress, may promote genotoxicity and cell cycle alteration, therefore conferring a higher hepatocarcinogenic potential to the AFB_1–FB_1 mixture.

ACKNOWLEDGMENTS

This study was supported by grants from Secretaría de Ciencia y Tecnología-Universidad Nacional de Córdoba; Agencia Nacional de Promoción Científica y Tecnológica (PICT 2010-1232, 2012-1742, 2013-0750, and 2015-2810). PAV hold fellowship from Agencia Nacional de Promoción Científica y Tecnológica. SLA hold fellowship from Secretaría de Ciencia y Tecnología-Universidad Nacional de Córdoba. VSM and SNO hold fellowships from the Consejo Nacional de Investigaciones Científicas y Técnicas (CONICET-Argentina). MGT is a career investigator of the latter institution.

We thank Paul Hobson, Ph.D., native speaker, for linguistic revision of the manuscript. The content of this work is the exclusive responsibility of their authors and does not necessarily represent the official views of the organisms that funded this research.

REFERENCES

[1] CAST. Mycotoxins: Risks in Plant, Animal, and Human Systems, Council for Agricultural Science and Technology Task Force report No. 139. Ames, Iowa, USA, 2003.

[2] Rodrigues I, Naehrer K. A three-year survey on the worldwide occurrence of mycotoxins in feedstuffs and feed. *Toxins (Basel).* 2012;4:663–675.

[3] Wagacha JM, Muthomi JW. Mycotoxin problem in Africa: current status, implications to food safety and health and possible management strategies. *Int J Food Microbiol.* 2008;124:1–12.

[4] Li FQ, Yoshizawa T, Kawamura O, Luo XY, Li YW. Aflatoxins and fumonisins in corn from the high-incidence area for human hepatocellular carcinoma in Guangxi, China. *J Agric Food Chem.* 2001;49:4122–4126.

[5] Sun G, Wang S, Hu X, et al. Co-contamination of aflatoxin B1 and fumonisin B1 in food and human dietary exposure in three areas of China. *Food Addit Contam A Chem Anal Control Expo Risk Assess.* 2011;28:461–470.

[6] Kensler TW, Roebuck BD, Wogan GN, Groopman JD. Aflatoxin: a 50-year odyssey of mechanistic and translational toxicology. *Toxicol Sci.* 2011;120(1):S28–S48.

[7] Shen HM, Ong CN, Lee BL, Shi CY. Aflatoxin B1-induced 8-hydroxydeoxyguanosine formation in rat hepatic DNA. *Carcinogenesis.* 1995;16:419–422.

[8] Diaz GJ, Murcia HW, Cepeda SM. Cytochrome P450 enzymes involved in the metabolism of aflatoxin B1 in chickens and quail. *Br Poult Sci.* 2010a;89:2461–2469.

[9] Diaz GJ, Murcia HW, Cepeda SM. Bioactivation of aflatoxin B1 by turkey liver microsomes: responsible cytochrome P450 enzymes. *Br Poult Sci.* 2010b;51:828–837.

[10] Gallagher EP, Kunze KL, Stapleton PL, Eaton DL. The kinetics of aflatoxin B1 oxidation by human cDNA-expressed and human liver microsomal cytochromes P450 1A2 and 3A4. *Toxicol Appl Pharmacol.* 1996;141:595–606.

[11] Guo Y, Breeden LL, Fan W, Zhao LP, Eaton DL, Zarbl H. Analysis of cellular responses to aflatoxin B(1) in yeast expressing human cytochrome P450 1A2 using cDNA microarrays. *Mutat Res.* 2006;593:121–142.

[12] Van Vleet TR, Macé K. Coulombe RA Jr Comparative aflatoxin B(1) activation and cytotoxicity in human bronchial cells expressing cytochromes P450 1A2 and 3A4. *Cancer Res.* 2002;62:105–112.

[13] Dohnal V, Wu Q, Kuca K. Metabolism of aflatoxins: key enzymes and interindividual as well as interspecies differences. *Arch Toxicol.* 2014;88:1635–1644.

[14] Liu L, Daniels JM, Stewart RK, Massey TE. In vitro prostaglandin H synthase- and monooxygenase-mediated binding of aflatoxin B1 to

DNA in guinea-pig tissue microsomes. *Carcinogenesis*. 1990;11: 1915–1919.

[15] Liu L, Massey TE. Bioactivation of aflatoxin B1 by lipoxygenases, prostaglandin H synthase and cytochrome P450 monooxygenase in guinea-pig tissues. *Carcinogenesis*. 1992;13:533–539.

[16] Roy SK, Kulkarni AP. Aflatoxin B1 epoxidation catalysed by partially purified human liver lipoxygenase. *Xenobiotica*. 1997;27:231–241.

[17] Hong Z, Jiang Z, Liangxi W, et al. Chloroquine protects mice from challenge with CpG ODN and LPS by decreasing proinflammatory cytokine release. *Int Immunopharmacol*. 2004;4:223–234.

[18] Kim CM, Kim JH. BMB reports: mini review; cytosolic phospholipase A2, lipoxygenase metabolites, and reactive oxygen species. *Biochem Mol Biol Rep*. 2008;41:555–559.

[19] Mary VS, Theumer MG, Arias SL, Rubinstein HR. Reactive oxygen species sources and biomolecular oxidative damage induced by aflatoxin B1 and fumonisin B1 in rat spleen mononuclear cells. *Toxicology*. 2012;302:299–307.

[20] IPCS-WHO. Fumonisin B1. Environmental Health Criteria 219. In: *International Programme on Chemical Safety (Ed.)*. Geneva: World Health Organization, 2000.

[21] Theumer MG, Canepa MC, Lopez AG, Mary VS, Dambolena JS, Rubinstein HR. Subchronic mycotoxicoses in Wistar rats: assessment of the in vivo and in vitro genotoxicity induced by fumonisins and aflatoxin B(1), and oxidative stress biomarkers status. *Toxicology*. 2010;268:104–110.

[22] Domijan AM, Abramov AY. Fumonisin B 1 inhibits mitochondrial respiration and deregulates calcium homeostasis-implication to mechanism of cell toxicity. *Int J Biochem Cell Biol*. 2011;43:897–904.

[23] Theumer MG, Clop PD, Rubinstein HR, Perillo MA. Effect of surface charge on the interfacial orientation and conformation of FB1 in model membranes. *J Phys Chem B*. 2012;116:14216–14227.

[24] Martinez-Larranaga MR, Anadon A, Diaz MJ, et al. Induction of cytochrome P4501A1 and P4504A1 activities and peroxisomal proliferation by fumonisin B1. *Toxicol Appl Pharmacol*. 1996;141:185–194.

[25] Mary VS, Valdehita A, Navas JM, Rubinstein HR, Fernandez-Cruz ML. Effects of aflatoxin B(1), fumonisin B(1) and their mixture on the aryl hydrocarbon receptor and cytochrome P450 1A induction. *Food Chem Toxicol*. 2015;75:104–111.

[26] Spotti M, Maas RF, de Nijs CM, Fink-Gremmels J. Effect of fumonisin B(1) on rat hepatic P450 system. *Environ Toxicol Pharmacol*. 2000;8:197–204.

[27] Meki ARM, Abdel-Ghaffar SK, El-Gibaly I. Aflatoxin B1 induces apoptosis in rat liver: protective effect of melatonin. *Neuroendocrinol Lett*. 2001;22:417–426.

[28] Ricordy R, Gensabella G, Cacci E, Augusti-Tocco G. Impairment of cell cycle progression by aflatoxin B1 in human cell lines. *Mutagenesis*. 2002;17:241–249.

[29] Stockmann-Juvala H, Savolainen K. A review of the toxic effects and mechanisms of action of fumonisin B1. *Hum Exp Toxicol*. 2008; 27:799–809.

[30] Ciccia A, Elledge SJ. The DNA damage response: making it safe to play with knives. *Mol Cell*. 2010;40:179–204.

[31] Singh R, Czaja MJ. Regulation of hepatocyte apoptosis by oxidative stress. *J Gastroenterol Hepatol*. 2007;22(1):S45–S48.

[32] Carlson DB, Williams DE, Spitsbergen JM, et al. Fumonisin B1 promotes aflatoxin B1 and N-methyl-N'-nitro-nitrosoguanidine-initiated liver tumors in rainbow trout. *Toxicol Appl Pharmacol*. 2001;172:29–36.

[33] Del Bianchi M, Oliveira CAF, Albuquerque R, Guerra JL, Correa B. Effects of prolonged oral administration of aflatoxin B1 and fumonisin B1 in broiler chickens. *Poult Sci*. 2005;84:1835–1840.

[34] Orsi R, Oliveira C, Dilkin P, Xavier J, Direito G, Correa B. Effects of oral administration of aflatoxin B 1 and fumonisin B 1 in rabbits (Oryctolagus cuniculus). *Chem Biol Interact*. 2007;170:201–208.

[35] Theumer MG, López AG, Aoki MP, Cánepa MC, Rubinstein HR. Subchronic mycotoxicoses in rats. Histopathological changes and modulation of the sphinganine to sphingosine (Sa/So) ratio imbalance induced by *Fusarium verticillioides* culture material, due to the coexistence of aflatoxin B1 in the diet. *Food Chem Toxicol*. 2008;46: 967–977.

[36] Sha B, Gao W, Wang S, et al. Oxidative stress increased hepatotoxicity induced by nano-titanium dioxide in BRL-3A cells and Sprague-Dawley rats. *J Appl Toxicol*. 2014;34:345–356.

[37] Sun LH, Lei MY, Zhang NY, et al. Individual and combined cytotoxic effects of aflatoxin B1, zearalenone, deoxynivalenol and fumonisin B1 on BRL 3A rat liver cells. *Toxicon*. 2015;95:6–12.

[38] Yiran Z, Chenyang J, Jiajing W, et al. Oxidative stress and mitogen-activated protein kinase pathways involved in cadmium-induced BRL 3A cell apoptosis. Oxid. *Med Cell Longev*. 2013;516051.

[39] Nicoletti I, Migliorati G, Pagliacci M, Grignani F, Riccardi C. A rapid and simple method for measuring thymocyte apoptosis by propidium iodide staining and flow cytometry. *J Immunol Methods*. 1991; 139:271–279.

[40] Aebi H. Catalase in vitro. *Methods Enzymol*. 1984;105:121–126.

[41] McLellan RA, Drobitch RK, Monshouwer M, Renton KW. Fluoroquinolone antibiotics inhibit cytochrome P450-mediated microsomal drug metabolism in rat and human. *Drug Metab Dispos*. 1996;24: 1134–1138.

[42] Gewert K, Sundler R. Dexamethasone down-regulates the 85 kDa phospholipase A2 in mouse macrophages and suppresses its activation. *Biochem J*. 1995;307:499–504.

[43] Araldi RP, de Melo TC, Mendes TB, et al. Using the comet and micronucleus assays for genotoxicity studies: A review. *Biomed Pharmacother*. 2015;72:74–82.

[44] Abdel-Wahhab MA, Hassan NS, El-Kady AA, et al. Red ginseng extract protects against aflatoxin B1 and fumonisins-induced hepatic pre-cancerous lesions in rats. *Food Chem Toxicol*. 2010;48: 733–742.

[45] Lin WC, Liao YC, Liau MC, Lii CK, Sheen LY. Inhibitory effect of CDA-II, a urinary preparation, on aflatoxin B(1)-induced oxidative stress and DNA damage in primary cultured rat hepatocytes. *Food Chem Toxicol*. 2006;44:546–551.

[46] Maynard S, Schurman SH, Harboe C, de Souza-Pinto NC, Bohr VA. Base excision repair of oxidative DNA damage and association with cancer and aging. *Carcinogenesis*. 2009;30:2–10.

[47] Dong H, Xu D, Hu L, Li L, Song E, Song Y. Evaluation of N-acetylcysteine against tetrachlorobenzoquinone-induced genotoxicity and oxidative stress in HepG2 cells. *Food Chem Toxicol*. 2014;64:291–297.

[48] Zafarullah M, Li WQ, Sylvester J, Ahmad M. Molecular mechanisms of N-acetylcysteine actions. *Cell Mol Life Sci*. 2003;60:6–20.

[49] Ehrlich V, Darroudi F, Uhl M, Steinkellner H, Zsivkovits M, Knasmueller S. Fumonisin B(1) is genotoxic in human derived hepatoma (HepG2) cells. *Mutagenesis*. 2002;17:257–260.

[50] Zhang F, Kong DS, Zhang ZL, et al. Tetramethylpyrazine induces G0/G1 cell cycle arrest and stimulates mitochondrial-mediated and caspase-dependent apoptosis through modulating ERK/p53 signaling in hepatic stellate cells in vitro. *Apoptosis*. 2013;18:135–149.

[51] Malumbres M, Barbacid M. Cell cycle, CDKs and cancer: a changing paradigm. *Nat Rev Cancer*. 2009;9:153–166.

[52] Shen X, Si Y, Wang Z, Wang J, Guo Y, Zhang X. Quercetin inhibits the growth of human gastric cancer stem cells by inducing mitochondrial-dependent apoptosis through the inhibition of PI3K/Akt signaling. *Int J Mol Med*. 2016;38:619–626.

[53] German OL, Miranda GE, Abrahan CE, Rotstein NP. Ceramide is a mediator of apoptosis in retina photoreceptors. *Invest Ophthalmol Vis Sci*. 2006;47:1658–1668.

[54] Riley T, Sontag E, Chen P, Levine A. Transcriptional control of human p53-regulated genes. *Nat Rev Mol Cell Biol*. 2008;9:402–412.

[55] Wang SK, Liu S, Yang LG, Shi RF, Sun GJ. Effect of fumonisin B(1) on the cell cycle of normal human liver cells. *Mol Med Rep*. 2013;7:1970–1976.

[56] Nagata Y, Partridge TA, Matsuda R, Zammit PS. Entry of muscle satellite cells into the cell cycle requires sphingolipid signaling. *J Cell Biol*. 2006;174:245–253.

[57] Spiegel S, Merrill AH. Sphingolipid metabolism and cell growth regulation. *FASEB J*. 1996;10:1388–1397.

[58] Meilhac O, Zhou M, Santanam N, Parthasarathy S. Lipid peroxides induce expression of catalase in cultured vascular cells. *J Lipid Res*. 2000;41:1205–1213.

[59] Aiken CT, Kaake RM, Wang X, Huang L. Oxidative stress-mediated regulation of proteasome complexes. *Mol Cell Proteomics*. 2011;10:-R110 006924.

[60] Grune T, Jung T, Merker K, Davies KJ. Decreased proteolysis caused by protein aggregates, inclusion bodies, plaques, lipofuscin, ceroid, and 'aggresomes' during oxidative stress, aging, and disease. *Int J Biochem Cell Biol*. 2004;36:2519–2530.

[61] Hwang ES, Kim GH. Biomarkers for oxidative stress status of DNA, lipids, and proteins in vitro and in vivo cancer research. *Toxicology*. 2007;229:1–10.

[62] Ayala A, Munoz MF, Arguelles S. Lipid peroxidation: production, metabolism, and signaling mechanisms of malondialdehyde and 4-hydroxy-2-nonenal. *Oxid Med Cell Longev*. 2014;360438.

[63] Ji C, Rouzer CA, Marnett LJ, Pietenpol JA. Induction of cell cycle arrest by the endogenous product of lipid peroxidation, malondialdehyde. *Carcinogenesis*. 1998;19:1275–1283.

[64] Niedernhofer LJ, Daniels JS, Rouzer CA, Greene RE, Marnett LJ. Malondialdehyde, a product of lipid peroxidation, is mutagenic in human cells. *J Biol Chem*. 2003;278:31426–31433.

[65] Ayed-Boussema I, Pascussi JM, Maurel P, Bacha H, Hassen W. Effect of aflatoxin B1 on nuclear receptors PXR, CAR, and AhR and their target cytochromes P450 mRNA expression in primary cultures of human hepatocytes. *Int J Toxicol*. 2012;31:86–93.

[66] Bui P, Solaimani P, Wu X, Hankinson O. 2,3,7,8-Tetrachlorodibenzo-p-dioxin treatment alters eicosanoid levels in several organs of the mouse in an aryl hydrocarbon receptor-dependent fashion. *Toxicol Appl Pharmacol*. 2012;259:143–151.

[67] Kinehara M, Fukuda I, Yoshida K, Ashida H. Aryl hydrocarbon receptor-mediated induction of the cytosolic phospholipase A2α gene by 2,3,7,8-tetrachlorodibenzo-p-dioxin in mouse hepatoma Hepa-1c1c7 cells. *J Biosci Bioeng*. 2009;108:277–281.

How to cite this article: Mary VS, Arias SL, Otaiza SN, Velez PA, Rubinstein HR, Theumer MG. The aflatoxin B_1-fumonisin B_1 toxicity in BRL-3A hepatocytes is associated to induction of cytochrome P450 activity and arachidonic acid metabolism. *Environmental Toxicology*. 2017;32:1711–1724. https://doi.org/10.1002/tox.22395